

Thermo-structural optimization of integrated thermal protection panels with one-layer and two-layer corrugated cores based on simulated annealing algorithm

Shu-yuan Zhao · Jian-jun Li · Chuan-xin Zhang ·
Wen-jiao Zhang · Xiu Lin · Xiao-dong He ·
Yong-tao Yao

Received: 19 August 2013 / Revised: 30 June 2014 / Accepted: 9 July 2014 / Published online: 8 August 2014
© Springer-Verlag Berlin Heidelberg 2014

Abstract To explore weight saving potential capability, a multidisciplinary optimization procedure based on simulated annealing algorithm was proposed to unveil the minimum weight design for integrated thermal protection system subjected to in-service thermal and mechanical loads. The panel configurations with one-layer and two-layer corrugated cores are considered for comparison. Heat transfer and structural field analysis for each panel configuration were performed to obtain the temperature, buckling, stress and deflection responses for structural components of interest, which were then considered as critical constraints of the optimization problem. Sensitivity analysis was performed to disclose the effect of individual design variables on the thermo-structural extreme responses, and the designed thermal protection system performance and weight for the two configurations were discussed. The results demonstrated that the two-layer structure provides superior structural efficiency and performance to resist thermal buckling deformation in comparison with the one-layer panel. Its area-specific weight is reduced by more than 14–29 % with respect to the one-layer panel design, and 30–50 % weight efficient can be implemented at higher thermal buckling constraint levels, while keeping considerable temperature, stress and deflection margins.

Keywords Integrated thermal protection system · Optimization · Corrugated · Simulated annealing · Design

1 Introduction

During the entire mission of Reusable Launch Vehicle (RLV), it is exposed to a superposition of severe environmental conditions and in-service loads, such as aerothermal, acoustic, small object high-speed impacts and inertial loads. Thermal protection system (TPS) is often used to protect a space vehicle from extreme reentry aerodynamic heating and also to provide an acceptable aerodynamic surface to prevent premature transition to turbulent flow during the atmospheric reentry. Although the primary function of a TPS is to maintain the vehicle structural temperature within acceptable limits, the operational capability and system weight also have significant impact on vehicle performance. To improve load-bearing capabilities and reduce weight of TPS, there has been great interest in the development of an integrated thermal protection system (ITPS) in recent years (Bapanapalli et al. 2006; Kumar et al. 2008; Ravishankar et al. 2011; Villanueva et al. 2010; Sharma et al. 2008). This concept provides an integrated structural component for thermo-mechanical load bearing as well as thermal protection function. The potential advantages of using such a structure over conventional TPS are its lower weight, lower maintenance, higher structural efficiency, larger panel sizes and multifunctional performance. One of the most suitable candidate structures for this purpose is a corrugated-core sandwich panel consisted of two thin face sheets and an inclined web core. The inner and outer face sheets carry the aerodynamic loading. The core helps stabilize the face sheets and supports shear loads through thickness. The corrugated core keeps the face sheets apart and stabilizes them

S.-y. Zhao (✉) · J.-j. Li · W.-j. Zhang · X. Lin · X.-d. He ·
Y.-t. Yao

Science and Technology on Advanced Composites in Special
Environments Laboratory, Harbin Institute of Technology,
Harbin 150080, China
e-mail: angel.zsy@126.com

C.-x. Zhang
Shanghai Engineering Center for Microsatellites,
Shanghai, 201203, China

by resisting vertical deformations, transverse shear strains, curvature in the longitudinal direction, and enables the structure to act as a single thick plate (Martinez 2007). The corrugated core will be filled with a non-load-bearing insulation to provide thermal protection through thickness of the system. All these characteristics make corrugated sandwich structures ideal for the development of ITPS, where weight, thermal protection and load bearing capability are important design criterion. The design of such a system is a challenging task since it involves many related technical disciplines. The structural requirements of robust members and thermal requirements of minimum heat conduction through the ITPS panel are often contradictory to one another in an overriding concern of weight.

There have been many researchers interested in the optimization issue of corrugated core sandwich panels in the past decades. Vinson et al. (1971, 1987) involved the determination of minimum weight web core composite material sandwich panel characteristics when the panel was subjected to uniaxial compression as well as both uniaxial compression and in-plane shear loads simultaneously. The involved failure modes include overstressing of the face and core material, overall panel buckling, buckling of the face and web core elements in compression (and shear). Liang et al. (2001) investigated the optimum design of metallic corrugated core sandwich panels subjected to blast loads by using a combined algorithm, in which the axial compression, bending and buckling constraints and the side constraints of manufacturing limitations on the sizes were considered. The effects of core configurations concerning the increase of structural stiffness for resisting blast loads and strength constraints along with the continuous and discrete design variables for optimization task were discussed. Tian et al. (2005) optimized corrugated panels subjected to uniform axial compression for minimum weight by using the naive optimization and SQP-based method. It was concluded that the simple naive optimization can only be applied to panels with simple geometries where the total number of design parameters does not exceed that of design constraints. Daxner et al. (2007) discussed methods of improving corrugated paper designs by applying numerical sizing optimization methods for the reduction of area-specific weight of the board while maintaining a required buckling strength both on the level of local buckling of liners and fluting and on the level of global buckling of whole plates made from corrugated board. However, the non-linear nature of the optimization problem does not ensure the prediction of a true optimum in a strict, global sense. Khalkhali et al. (2007) designed the minimum-weight sandwich panels with periodic, open-cell corrugated cores using genetic algorithm, observing yielding and buckling in components as optimization constraint. Analytical expressions for critical loads were derived, and then minimum weights for

some load capacities were determined. For evaluating optimized values, the obtained results by analytical method and finite element method were compared. In view of the above-mentioned research, only mechanical loads were considered in the design of corrugated sandwich panels. However, large temperature gradient between the top and bottom face sheet, which is one of the most severe loads influencing the design of ITPS panels, has not been considered in their optimization procedures. Bapanapalli et al. (2006, 2007) developed an optimization procedure for finding the optimal geometry leading to minimum mass design of ITPS panel with one-layer corrugated core sandwich ITPS structure. The procedure used finite element analyses to construct response surface approximations (RSA) of the critical constraints, including temperature, stress, deflection and buckling. The weight and geometric parameters in describing the sandwich structure were optimized through a Matlab function *fmincon*(). Gogu et al. (2009) did minimal weight design and comparison study by choosing more suitable materials for further lowering the ITPS mass. However, it is expected that there is high potential to realize the weight-loss purpose by optimizing configuration of cross-sections for ITPS panel.

To improve structural efficiency and reduce structural weight, more competitive ITPS panel concept and its corresponding multidisciplinary design optimization technique should be proposed. For validation and comparison purposes, in the presented work, we use the same materials, thermo-mechanical loads and boundary conditions, objective and constraint functions, and design variables ranges which were used in Bapanapalli's work of ITPS design, since we have identical motivation for thermal protection application. The main innovation and difference between this work and the Bapanapalli's work (Bapanapalli et al. 2006; Bapanapalli 2007) as well as others are threefold. The first is to provide a two-layer corrugated ITPS panel configuration, along with a discussion on weight-loss feasibility of this two-layer structure for ITPS applications. Second, taking into account the non-linear nature of the optimization problem, simulated annealing algorithm is proposed to fulfill the multidisciplinary design optimization process of the provided structures in order to obtain a global optimization result. Though it is a commonly used optimization technique, application in the design of these kinds of thermo-mechanical structures is still scarce. Third, the designed ITPS performance and weight for one-layer and two-layer corrugated configurations are compared on the basis of validation of the developed optimization model, and effects of panel configurations with different cores on the thermo-structural response behaviors and reduction of structural weight are discussed.

The rest of this manuscript is structured as follows: In the next section, a detailed description about the optimization

problem of the proposed ITPS panels is introduced, including the design variables, objective function and constraint function of optimization. In Section 3, the thermo-structural analysis methods of the panels are briefly presented. Following these thermo-structural analysis, approximated response surfaces between the structural responses and design variables are constructed by Latin-Hypercube sampling and regression analysis techniques in Section 4. In Section 5, the simulated annealing algorithm and multi-disciplinary design optimization procedure to determine the minimal mass for the two corrugated-core sandwich ITPS panels are provided. After the validation of thermo-structural analysis, RSA and optimization models in section 6, thermo-structural extreme responses sensitivity and designed ITPS performance and weight for the two corrugated configurations are discussed in Section 7. Finally, the conclusions and final remarks are presented in Section 8.

2 The optimization problem statement

Two corrugated core sandwich configurations for potential use in ITPS for future space vehicles will be investigated in this paper. The first configuration, shown in Fig. 1a, consists of one layer of corrugated core element sandwiched

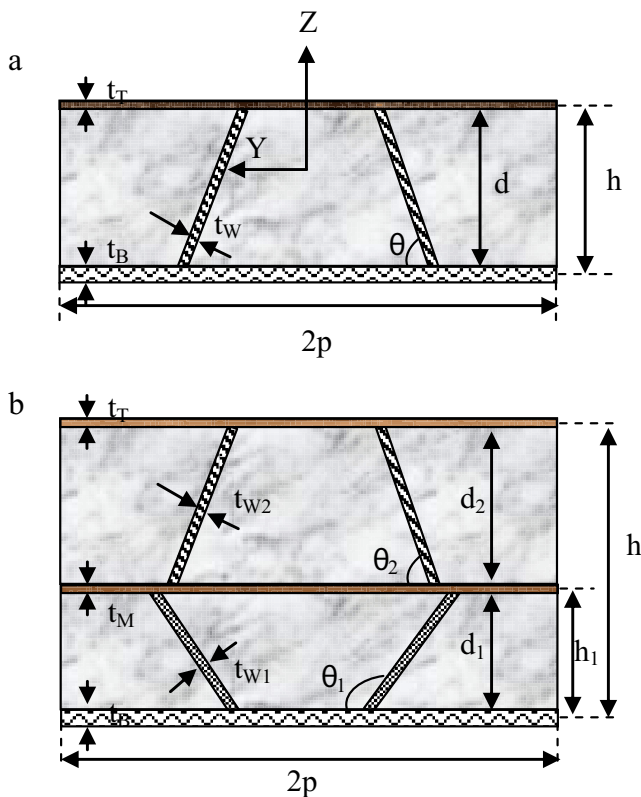


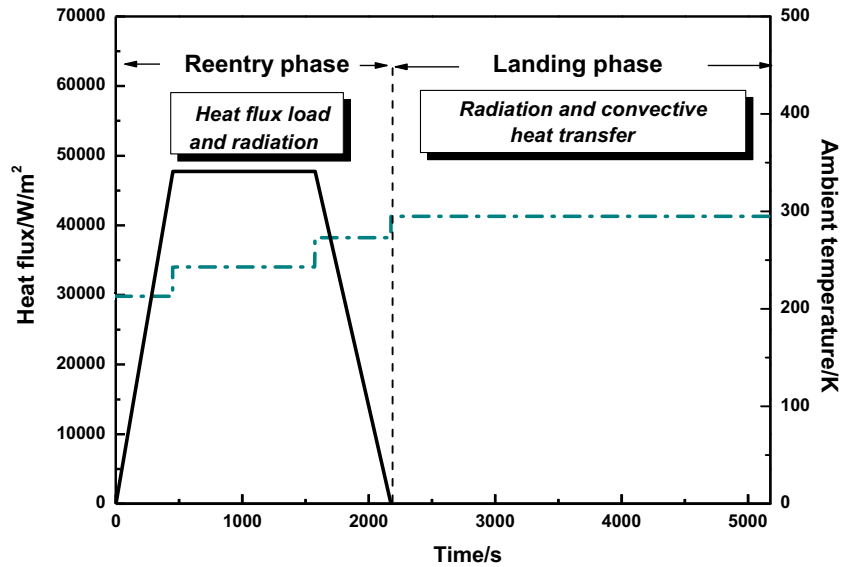
Fig. 1 The configuration of one-layer (a) and two-layer (b) corrugated core sandwich panel

between the outer and inner face sheets. The second configuration, shown in Fig. 1b, consists of two layers of corrugated core between face sheets. A medium sheet separates the two layers of corrugated core elements. Fibrous ceramic insulation is filled inside the corrugated core space to block heat flow from top to bottom face sheet. The relevant geometric variables of the ITPS design are also shown on the unit cell in Figs. 1. For the one-layer configuration, these variables are the thickness of top face sheet (TFS) t_T , web sheet (WEB) t_W and bottom face sheet (BFS) t_B , the height of panel h and web core d , the corrugation angle θ , and the length of unit cell $2p$. For the two-layer one, the additional variables in describing the configuration are the medium face sheet (MFS) thickness t_M , the height of bottom core panel h_1 , the height of bottom web core (B-WEB) d_1 and top web core (T-WEB) d_2 , the web thickness of bottom core t_{W1} and top core t_{W2} , the corrugation angle of bottom core θ_1 and top core θ_2 . For the sake of simplicity, it is assumed that length of unit cell of the top core is the same as that of the bottom core for the two-layer panel.

The ITPS panel is subjected to various combinations of mechanical and thermal loads such as pressure, thermal flux, temperature, in-plane impact loads and acoustic loads during service. For this paper, heat loads, aerodynamic pressure loads and in-plane inertial loads on the ITPS panel are considered as the critical loads. The heat loads imposed on the structure are schematically illustrated in Fig. 2 (Bapanapalli 2007). During reentry phase (before 2175s), the top surface has incident heat flux loading and radiation boundary conditions. After the vehicle lands (after 2175s), there is no heat input and the top surface has radiation and convective heat transfer boundary conditions. The pressure load is equal to zero before landing and is equal to 1 atmosphere after landing. Another mechanical load on the ITPS is the in-plane inertial compression load. This in-plane load of 30,000 N/m is only applied during reentry phase. After landing, no in plane load is applied on the ITPS.

ITPS panel is a multi-functional structure that combines conventional heat shield and load bearing structural functions required for a hypersonic vehicle. Because of its complex design, an ITPS panel could fail due to multiple failure modes depending on the sandwich geometry, load and boundary condition. For the current analysis, the time when the maximum temperature difference between the top face sheet and bottom face sheet occurs is considered as the most critical time, and the following four critical constraints are taken into account: 1) the temperature of underlying structure must be maintained below acceptable limits at all times. Thus, peak bottom surface temperature is an important design driver; 2) though local buckling responses of the ITPS structure made of thin plates are not catastrophic, they may lead to other failures in postbuckling load range. Therefore, the thermal/mechanical buckling

Fig. 2 The heat loads imposed on the corrugated core sandwich panels



is another major design driver; 3) to maintain structural integrity, the stresses in the panel should be within allowable limits; 4) limits on the deflection of the top surface are imposed to prevent boundary-layer transition at high Mach numbers and to prevent permanent compaction of fibrous insulation.

In order to minimize operational costs, a TPS should be as lightweight as possible while fulfilling all the required thermal protection and load-bearing functions of an ITPS. To reconcile various conflicting requirements, an optimization process is needed to find a feasible solution. The optimization problem can be described as the weight minimization of two configuration panels under the given loading conditions while satisfying all the constraints such as temperatures, buckling, stresses and deflections limits in various parts of the structure. The design variables for the optimization are the geometry parameters of a unit cell, i.e. $X_1 = \{t_T, t_B, t_W, \theta, h, p\}$ and $X_2 = \{t_T, t_M, t_B, t_{W1}, t_{W2}, \theta_1, \theta_2, h, h_1, p\}$ for the one-layer and two-layer configurations, respectively.

The mass per unit area as objective function for the one-layer ITPS panel can be described as:

$$f_1(X_1) = \rho_T t_T + \rho_B t_B + \rho_W t_W d / (p \sin \theta) + \rho_S d (1 - t_W / (p \sin \theta)) \tag{1}$$

and for the two-layer panel

$$f_2(X_2) = \rho_T t_T + \rho_M t_M + \rho_B t_B + \rho_{W1} t_{W1} d_1 / (p \sin \theta_1) + \rho_S d_1 (1 - t_{W1} / (p \sin \theta_1)) + \rho_{W2} t_{W2} d_2 / (p \sin \theta_2) + \rho_S d_2 (1 - t_{W2} / (p \sin \theta_2)) \tag{2}$$

with $d = h - (t_T + t_B)/2$, $d_1 = h_1 - (t_M + t_B)/2$, $d_2 = h - h_1 - (t_M + t_T)/2$.

Where $\rho_T, \rho_B, \rho_W, \rho_M$ and ρ_S are densities of the top face sheet, bottom face sheet, web, medium sheet material and insulation material, respectively.

The constraint functions for the two configurations are given as:

$$Max(T_{BFS}) \leq T_{Lim} \tag{3a}$$

$$Min(\lambda) \geq \lambda_{Lim} \tag{3b}$$

$$Max(\sigma) \leq \sigma_{Lim} \tag{3c}$$

$$Max(D_{TFS}) \leq D_{Lim} \tag{3d}$$

where T, λ, σ and D are the temperature, buckling eigenvalue, von Mises stress and deflection of the panel, respectively. The subscript Lim represents the allowable limits.

3 Thermo-structural analysis of the two configuration panels

To obtain the thermo-structural responses required for the design constraints of such ITPS panels, heat transfer and structural field analysis is performed. For the current analysis, the bottom face sheet for the considered two panels is made of a beryllium alloy, with its density of 1855 kg/m³ and Poisson’s ratio of 0.063. Titanium alloy (Ti-6Al-4V) is used for the top (and medium) face sheet as well as the web core and its density and Poisson’s ratio are 4429 kg/m³ and 0.31, respectively. The core of the sandwich panel is assumed to be filled with Saffil fibrous insulation with the density of 24 kg/m³. The remaining temperature dependent thermophysical and mechanical properties

of the materials used for the panels are taken from Ref. Bapanapalli (2007).

3.1 Thermal analysis

One of the goals of performing a transient heat transfer analysis is to determine the maximum bottom face sheet temperature, which is required for the temperature constraint. Another goal is to identify the critical time of maximum thermal gradient and provide the temperature distribution along thickness of the panel at that critical time, which will act as thermal loads for the structural analysis.

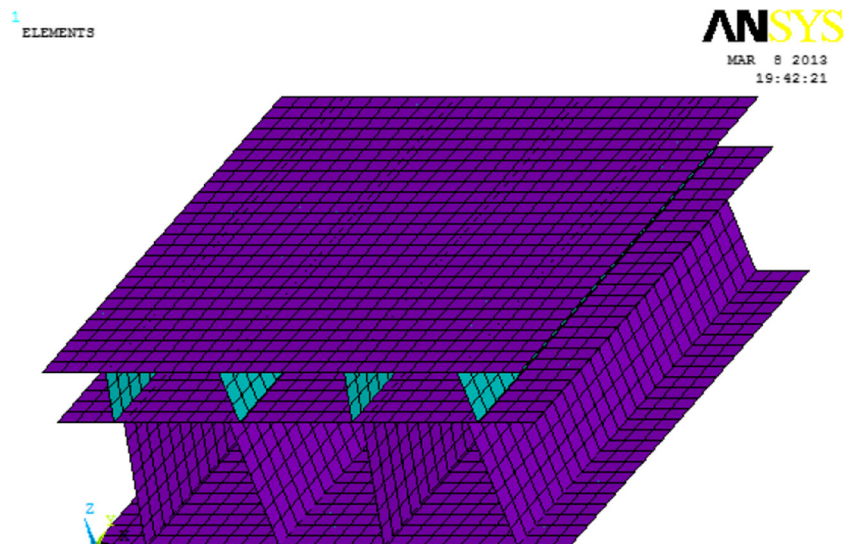
The model developed by Bapanapalli (2006) is used to describe heat transfer of ITPS panel. A brief description of the heat transfer models of ITPS is given in Appendix A. The panel is subject to an incident heat flux assumed to vary as shown in Fig. 2. Re-radiation condition and convective heat loss are applied on the top surface. The bottom surface is assumed to be adiabatic boundary condition. It has been shown that such a one dimensional heat transfer model can accurately predict the temperature distribution through the thickness of the sandwich panel in Ref. Bapanapalli et al. (2006). The heat transfer equations of ITPS are solved numerically using an implicit, transient, one-dimensional (1-D) finite difference technique, and the temperature response at each time and each location can be easily obtained.

3.2 Thermal buckling, stress and deflection analysis

To determine the mechanical constraints required for optimum design of the two proposed ITPS configurations, the thermal buckling, thermal stress and deflection analysis will be carried out using ANSYS finite element software package.

In the finite element model, only the solid portions of the ITPS panel which include the face sheets and webs, is taken into account. The insulation is a kind of soft, flexible cotton wool material with nearly no mechanical properties compared with the properties of other solid materials that make up the ITPS panel, especially for such a low density (24 kg/m^3) material. It is hard to be considered as a structural member in previous analysis and design of thermal protection system (Bapanapalli et al. 2006; Poteet et al. 2004; Pichona et al. 2009). Therefore, the insulation is omitted from all thermo-mechanical structural analyses. Taking into account the symmetry of the structure, a one-quarter symmetric representation is considered to reduce the number of degrees of freedom at the development stage of model. Four-node SHELL 181 elements with 6 degrees of freedom are used in the modeling of the face sheets and corrugated core sheets. The rigid constraint at the interfaces between the face sheets and corrugated core sheets is modeled by multipoint constraint MPC184 elements. An example of mesh is depicted in Fig. 3, and around 7852 elements are used for the given finite element model. The boundary conditions at the panel edges considered are 1) fixed z-direction displacements of the BFS, and only fixed three rotations of the TFS on the actual edges of the panel; 2) fixed displacements in the direction vertical to symmetric surface and fixed other two directions rotations on the symmetric edges of the FE model. The loads in the stress, deflection and buckling FE analyses include temperature, aerodynamic pressure and in-plane compression loads. The temperature distributions through thickness at the critical reentry time obtained from the heat transfer analysis is imposed to each node of the mesh in terms of its z-coordinates. The pressure load is imposed on the top surface, while the in-plane load is applied only in the y-direction of bottom face sheet of panels.

Fig. 3 Typical FE shell element mesh for buckling analysis



The thermal buckling behavior of different sections of the ITPS panel was probed by running a set of FE elastic buckling analyses (eigenvalue extractions) using the developed models. For this research, the first 100 smallest eigenvalues and the corresponding eigenvectors were extracted through ANSYS finite element analysis. From these values the smallest positive eigenvalue for each component of panel was obtained separately.

The thermal stress and static deflection analysis of the sandwich panels due to thermal gradients and mechanical loads was also performed. From the analysis models, the z-direction deflection of the top face sheet and the von Mises stress for each section of the ITPS can be obtained from the ANSYS output files.

4 Response surface approximations for thermo-structural responses

During the optimization design process, hundreds of thermo-structural analysis has to be performed to obtain responses of thermal, buckling, stress and deflection constraints. The calculation of response data points by direct finite element analyses would be computationally expensive. To release the computational burden, many surrogate modeling methods are usually employed to generate surrogates of the computationally expensive simulation-based models such as Kriging models (Martin and Simpson 2005), support vector regression (Clarke et al. 2005), Artificial Neural Networks (Hastie et al. 2001), polynomial based Response Surface Approximations (RSA) (Myers and Montgomery 1995), etc In this research, a quadratic response surface approximation, provided in Appendix B, is used to construct each constraint as functions of the design variables of the considered structures, since this method is simple, easy to implement and has reasonable accuracy for concept and preliminary design of structure. To avoid the variables being clustered in any region of the design space, plain Latin Hypercube Sampling (LHS) technique was used for the design of experiments. In the plain Latin Hypercube scheme, each of variable ranges is divided into N (the number of sampling) equally spaced intervals. The values per variable are randomly selected from each of these N intervals and then combined to form an experimental design points. N different combinations of the design variables are obtained through repeated sampling. For the one-layer corrugated sandwich panel, a quadratic RS approximation in 6 variables has 28 coefficients and 150 function evaluations are used to determine all the coefficients. For the two-layer configuration, there are 10 design variables and 65 coefficients. Therefore, a total of 500 Latin hypercube sample points were input to the finite element analyses to generate fairly accurate response surfaces approximations

for the design process. To improve accuracy of fitted function, the response surfaces was fitted separately for different components of ITPS panels in the previous research work (Bapanapalli et al. 2006). Though this method is efficient for the one-layer structure, no obvious improvement is observed for thermal buckling response approximation of the two-layer structure, due to large scatter of response values and large number of the design variables. Hence, in this research, piecewise fitting concept is employed. We firstly identified two design variables (variable A and B) which give the most important influence on the response based on the sensitivity analysis (see in Appendix C and Section 7.1). And then, each non-dimensional variable is divided into two intervals at its mean value, i.e. $X_A : [0, 0.5) \cup [0.5, 1]$ and $X_B : [0, 0.5) \cup [0.5, 1]$. After that, the domain constituted with the two identified variables can be divided into three regions: variable domain (e.g. $X_A \in [0, 0.5), X_B \in [0, 0.5)$) which has a positive impact on the response, variable domain (e.g. $X_A \in [0.5, 1], X_B \in [0.5, 1]$) which has a negative impact on the response, and the remaining domain (e.g. $X_A \in [0.5, 1], X_B \in [0, 0.5)$ and $X_A \in [0, 0.5), X_B \in [0.5, 1]$). Finally, the response surface between extreme response and design variables for different domains was constructed separately using regression analysis method (Xu 2004). The variables are rejected or accepted at the significance level of 0.25. In the above-mentioned method, the high and low values of extreme response are partitioned in different domains determined by two most influential variables, which significantly reduces the variation range of responses in one fitting. Therefore, better fitting results would be obtained.

5 Optimization by simulated annealing algorithm

In the present study, we attempt to develop a procedure that can locate global optimum designs with minimum mass per unit area of the corrugated sandwich panels while satisfying all the thermal and mechanical constraints in various parts of the structure in a given design space. For this purpose, classical optimization techniques, based on the calculation of derivatives, are excluded in these problems, since they have the risk to be trapped in a local optimum. For global optimization issue, the most commonly used methods include Genetic Algorithm (GA) (Aryanezhad and Hemati 2008), Particle Swarm Optimization (PSO) (Kumar et al. 2008) and simulated annealing algorithm (Alrefaei and Diabat 2009; Kirkpatrick et al. 1983; Metropolis et al. 1953). It was reported that the GA and PSO methods may have deficiencies of premature convergence (Shi and Eberhart 1998; Shieh et al. 2011), which would degrades their performances by reducing their search capability. In this respect, simulated annealing method exhibits superior robustness

and global searching capability, which has been successfully used for many global structural optimization problems with multiple local optima (Savsani et al. 2010; Lombardi et al. 1992; Erdal and Sonmez 2005). This method is inspired from the thermodynamic process of annealing of molten metals to attain the lowest free energy state (Kirkpatrick et al. 1983). The key principle of the method is to allow occasional worsening moves so that these can eventually help locate the neighborhood to the global minimum according to the Metropolis criterion (Metropolis et al. 1953). For the current problem, the simulated annealing based optimization design cycle we employed is shown below.

- 1) Starting from an initial design and given initial temperature of 4000, final temperature of 0.0001, temperature reduction factor, number of search points in a temperature of 50, and convergence criterion.
- 2) A new design is randomly generated in the design space by applying a small perturbation to the current one.
- 3) Calculate the objective function value at the new design point and compared with the current objective function value. If the new objective function value is less than the current value, the new design updates the current one. Otherwise it is rejected, unless an acceptance probability P is greater than a generated random number between zero and one.
- 4) The algorithm is terminated when the final annealing temperature is less than 0.0001, or the reduction rate of the objective function value for two consecutive temperatures is less than 0.00001
- 5) At the end of the cycle the temperature is updated, and the cycle is repeated until the optimization is stopped by the stopping criterion.

To speed up the optimization convergence, Harold et al. (1987) developed a SA algorithm called Fast Simulated Annealing (FSA). FSA uses the state generator with Cauchy distribution to replace the state generator with Gaussian distribution used in the classical SA. In previous research (Harlod and Hartley 1987; Mageras and Mohan 1993; Wang and Zheng DZ 2000), a detailed performance comparison of the above two generators was made. It was concluded that the Cauchy distribution implies an occasional long jump among local minimum more easily than Gaussian distribution, and then of course speed up the optimization convergence. In the FSA, the design variables are updated at each annealing time as follow:

$$x_i^{t'+1} = x_i^{t'} + y_i (UB_i - LB_i) \quad (4)$$

Where t' is the time index for the annealing process, x_i is the i th design variable and $x_i \in [LB_i, UB_i]$, UB_i and LB_i are the upper and lower bounds of the x_i , respectively. $y_i \in [-1, 1]$ and y_i is the random variable generated by the

following generating function

$$y_i = T_{SA} \operatorname{sgn}(u - 0.5) \left[(1 + 1/T_{SA})^{|2u-1|} - 1 \right] \quad (5)$$

Where u is a uniformly distributed random number on $[0, 1]$, $\operatorname{sgn}(x)$ is the sign function, and T_{SA} is the temperature controlling the optimization process.

The acceptance probability is classically given by the Boltzmann probability, viz.

$$P = \exp\left(\frac{-\Delta E}{K_B T_{SA}}\right) \quad (6)$$

where ΔE is the change in the energy value from one point to the next, K_B is the Boltzmann's constant.

For this application, a geometric cooling schedule, namely $T_{SA-new} = 0.95T_{SA-old}$, is adopted. During the optimization process using SA, the penalty function approach is utilized to treat the constrained problems. By adding a penalty term to the objective function, the constrained problem is transformed into unconstrained one.

6 Validation of thermo-structural analysis, RSA and optimization models

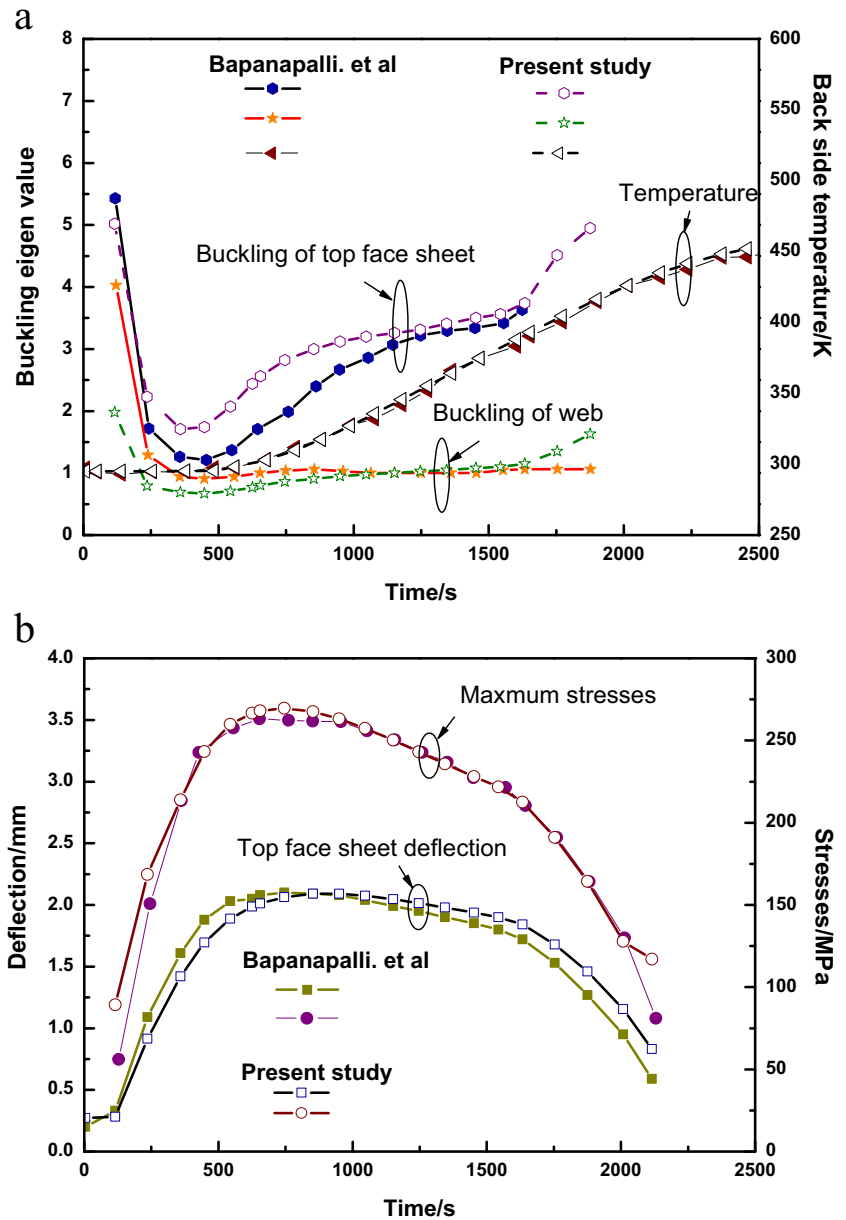
Before the proposed methods are used for optimization design of ITPS panel, various levels of validation are needed to guarantee the reliability of the developed models. In this section, the thermal, thermo-mechanical and optimization design analysis are performed to verify the developed models. The obtained results were compared with the results provided by Bapanapalli (2007) for the one-layer ITPS panel. At the same time, the accuracy of RSA fitted models is also checked. The values of the geometric parameters used for the validation are given in Table 1.

Figure 4 shows the variations of the temperature on the BFS, the smallest thermal buckling eigenvalues, the maximum stresses as well as the deflection of TFS with reentry time. As can be seen from the figures, both the results in Ref. Bapanapalli (2007) and our results in the temperature response on the BFS, maximum stresses and deflection of the TFS correspond very well, as the maximum average difference is less than 9 %. The smallest thermal buckling eigenvalues exhibit large deviations, and the average difference between them is about 16 %. Considering that the selected properties of material, element type and size of finite element model all have effects on the calculated results, we think this difference is acceptable.

Table 1 The values of geometric parameters used for the validation

Parameters	t_T , mm	t_B , mm	t_W , mm	θ , °	d , mm	p , mm
Value	1.2	3.84	1.01	100.0	101.9	56.25

Fig. 4 Comparison of predicted responses with respect to reentry time in present study with the results provided by Bapanapalli (2007) the temperature on the BFS and the smallest thermal buckling eigenvalues (a), the maximum stresses and the deflection of the TFS (b)



The quality of constructed response surface of temperature, thermal stress and deflection, and thermal buckling constraints for one-layer and two-layer corrugated structures is summarized in Tables 2 and 3, respectively. The ‘R’

in these tables stands for the coefficient of multiple determination of fitted function. The ‘RMSE-D %’ stands for percentage of the root mean square error of design points when compared to their average value of response. The

Table 2 Accuracy of the constructed response surfaces for one-layer ITPS optimization

Constraints	Min	Max	Mean	R	RMSE-D %	RSME-T %
Temperature (K)	378.06	672.53	466.95	0.99	0.71	0.57
Deflection (mm)	0.72	7.70	2.95	0.99	3.76	2.34
Max. stress of TFS and WEB (MPa)	103.80	757.79	392.60	0.99	4.75	4.39
Max. stress of BFS(MPa)	90.20	437.25	264.70	0.99	4.22	3.41
Min. buckling eigenvalue of TFS	0.29	59.38	5.40	0.97	12.97	11.36
Min. buckling eigenvalue of WEB	0.24	4.39	1.13	0.98	8.70	9.13

Table 3 Accuracy of the constructed response surfaces for two-layer ITPS optimization

Constraints	Min	Max	Mean	R	RMSE-D %	RSME-T %
Temperature (K)	364.78	652.07	456.67	0.99	0.73	0.57
Max. stress of BFS(MPa)	10.70	274.10	72.53	0.95	18.36	14.25
Min. buckling eigenvalue of TFS	0.38	127.85	8.71	0.94	25.64	18.86
Min. buckling eigenvalue of T-WEB	0.27	167.90	6.94	0.94	30.79	23.51
Min. buckling eigenvalue of MFS	0.88	127.85	6.46	0.95	23.96	20.52
Min. buckling eigenvalue of B-WEB	0.25	133.57	6.92	0.96	19.85	17.71

'RMSE-T %' stands for percentage of the root mean square error of testing points when compared to the average response value of design points. The determination method for 'R', 'RMSE-D %', and 'RMSE-T %' values is provided in Appendix B. The response surfaces for all the constraints of one-layer ITPS panel have very high coefficient of multiple determination R which indicate good prediction capabilities. The 'RMSE-D %' and 'RMSE-T %' for the constructed response surfaces are less than about 13 % in all cases. Since the extreme response values in the top face deflection and stress of the top and medium face sheets and webs of two-layer panel are far less than the design allowable value, only the response surface accuracy of the active constraints in the optimization is given, and shown in Table 3. For the two-layer structure, the temperature response surface has been found to be highly accurate. However, the thermal buckling eigenvalue response surface shows large error between the actual and predicted values of design points. This deviation may be due to a large variation observed in the buckling eigenvalues at different design points, which decreases the accuracy of the response surface approximations. Advanced surrogate modeling techniques may be more efficient to improve the accuracy of the design response surface. It is worthwhile to highlight the fact that the present research is to discuss the weight-loss feasibility of two-layer corrugated ITPS

structures at the concept design and preliminary design phase. The improvement of accuracy for the given concept would be the main task of the third phase of design (The design phase usually includes concept design, preliminary design, and detail design phase). Therefore, in spite of the large errors, the response surface approximations can be expected to be qualitatively reasonable and can be used for the design process.

The optimum design for the one-layer panel was also performed using the response surface approximation and simulated annealing technique for validation of the optimization proposal. A maximum allowable bottom surface temperature of 473 K, a smallest allowable buckling eigenvalue of 1.25, a maximum allowable safety factor satisfying the maximum stress theory of 1.2, and a maximum allowable top surface deflection of 6 mm were included. The yield stresses of titanium alloy and beryllium alloy used for the analysis are 620 MPa and 290 MPa, respectively. The ranges of the geometric parameters and the optimized design results in comparison with the results in Ref. Bapanapalli (2007) are given in Table 4. Instead of the length of the whole panel and the number of unit cell, the length of unit cell is considered as design variable for the current analysis. We made minor conversion to these design variables (the length of unit cell is the ratio of the length of whole panel and the number of unit cell). From the results, it is demonstrated

Table 4 The ranges of geometric parameters and the optimized design results in comparison with the results in Ref. Bapanapalli (2007)

Ref. Gogu et al. (2009), Opt. 1-4	Opt.1	Opt.2	Opt.3	Opt.4	Present study
t_T (1-2mm)	1.2	1.2	1.32	1.2	1.18
t_B (2-8mm)	3.84	7.49	5.49	7.75	5.08
t_W (1-2mm)	1.01	1.63	1.36	1.62	1.26
θ (80–100°)	100	80	100	80	99.99
h (80-1-20mm)	101.9	80	120	83.82	81.19
L (450-900mm)	450	682.9	450	496.9	–
n (4–10)	4	10	6	8	4
$p=L/2n$ (22.5–112.5mm)	56.25	34.145	37.5	31.056	64.01
Mass kg/m^2	23.658	40.028	40.770	43.596	23.406
Actual $Max(T_{BFS})$ (K)	457.93	–	–	–	468.55
Actual $Max(\sigma_{Be})$ (MPa)	259.12	–	–	–	257.29
Actual $Min(\lambda)$	0.98	–	–	–	1.13

Table 5 The ranges of geometric parameters for the design of the one-layer configuration

Parameters	t_T , mm	t_B , mm	t_W , mm	θ , $^\circ$	h , mm	p , mm
Range	1–2	2–8	1–2	80–100.0	80–120	22.5–112.5

that the designed geometric parameters for this research are within the range of five design points presented in Ref. Bapanapalli (2007). The current designed weight is very close to the lightest design results with four unit cells in Ref. Bapanapalli (2007). The actual response values of the active constraints for the current design and the lightest design in Ref. Bapanapalli (2007) are also shown in Table 4. The generally good behavior demonstrates that the provided multidisciplinary optimization models are fairly accurate and can be relied upon.

7 Results and discussion

As mentioned above, hundreds of thermo-structural analysis was performed to obtain response data points which were then used for construction of the response surface approximation. To extract more useful information for the structural design and RSA construction from the response data, we performed a sensitivity analysis. And then the optimization design results for the two configurations were discussed. In this study, the ranges of the geometric parameters used for the design of the one-layer and two-layer core configurations are the same as that provided in Ref. Bapanapalli (2007), and given in Tables 5 and 6, respectively. It should be mentioned that the lower bound of the bottom and top core height is supposed to be 5 mm during the design process of the two-layer panel, considering the manufacturing limitations on the sizes.

7.1 Thermo-structural extreme responses sensitivity analysis

To gain good insight into the responses mechanism and facilitate the subsequent optimum design, the correlation coefficient method was employed to roughly gauge the contributions of each geometric parameter to the thermo-structural extreme responses. A brief description of correlation coefficient method (Miller et al. 1965) is given in

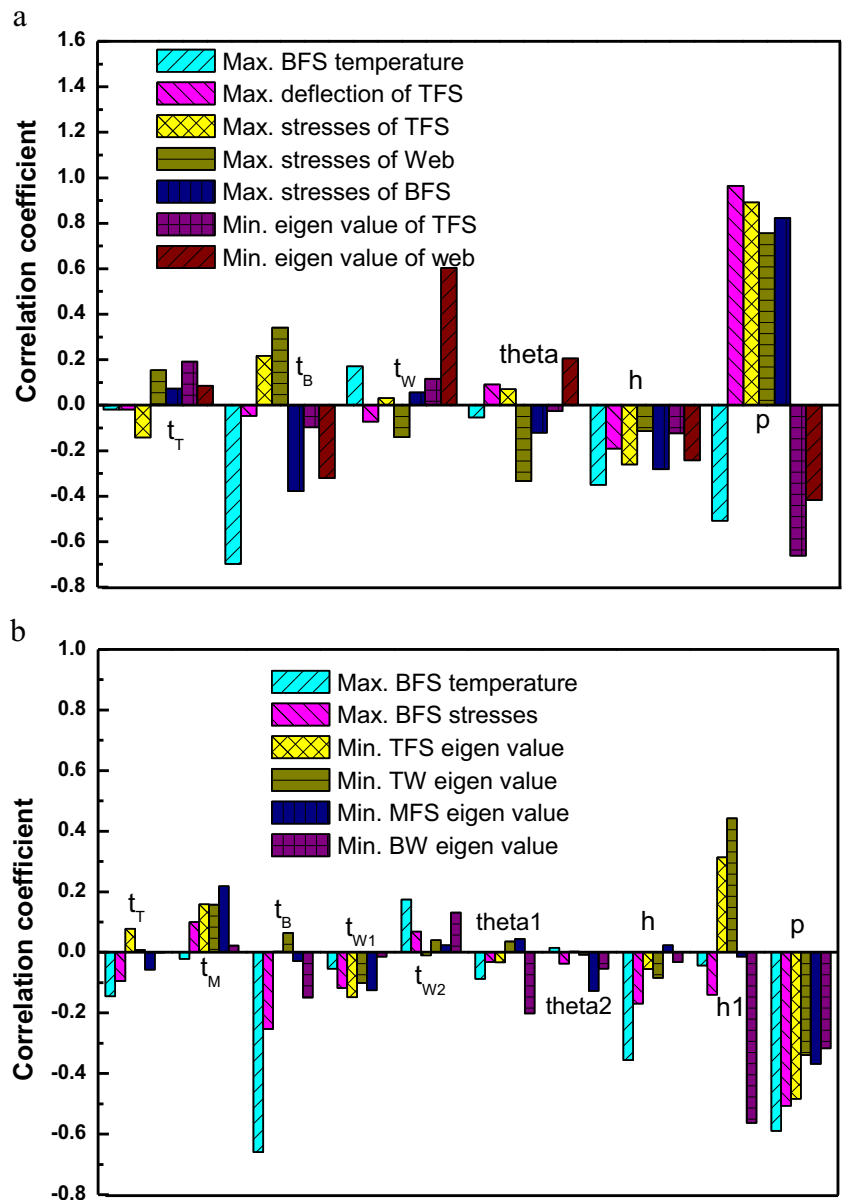
Table 6 The ranges of geometric parameters for the design of the two-layer configuration

Parameters	t_T , mm	t_M , mm	t_B , mm	t_{W1} , mm	t_{W2} , mm
Range	1–2	1–2	2–8	1–2	1–2
Parameters	θ_1 , $^\circ$	θ_2 , $^\circ$	h , mm	h_1 , mm	p , mm
Range	80–100	80–100	80–120	5–(h-5)	22.5–112.5

Appendix C. The calculated correlation coefficients for the one-layer and two-layer ITPS panels are shown in Fig. 5a and b, respectively. As can be seen from Fig. 5a, the length of unit cell p has significant effect on all the thermo-structural extreme responses. With the increase of the p value, the maximum temperature of the bottom face sheet and the minimum thermal buckling eigenvalue decrease, and the maximum thermal stress and the maximum deflection of the top face sheet increase. The changes in the buckling eigenvalue, stress and deflection may have negative impact on the structural safety. However, large unit cell length is favorable to the extreme temperature response which makes the panel gain more thermal safety margin. Increasing the height of panel h is helpful to decrease temperature, stress and deflection for the structural components of interest, but higher panel is susceptible to thermal buckling. The values of t_B and t_W have greater positive impact on the extreme temperature and buckling eigenvalue of web, respectively. The t_T seems to have little effect on the extreme responses for the current considered range of design variables, indicating that this parameter may not be an important design factor.

Since the extreme response values in the top face deflection and stress of the top and medium face sheets and webs of two-layer panel are far less than the design allowable value, only the effects of design parameters on the temperature, stress on BFS and buckling extreme responses are plotted in Fig. 5b. The length of unit cell p is still the most important design parameter, and all the extreme thermal and buckling responses are reduced with the increase of this parameter. It is interesting to notice that the h_1 became to be more important parameter in effecting the thermal buckling than the web thickness. The higher bottom web core, the smaller buckling eigenvalue of bottom web, and the larger eigenvalues of top face sheet and top web. The θ_1 has non-negligible effect on the thermal buckling of the bottom web. In addition to p , the value of t_B has considerable influence on the stress of BFS. With its increase, the deformation resistance by the bottom face sheet is much higher because it is the thickest section of the panel and thus leads to this reduction of thermal stress. The maximum back side temperature decreases with the rise of t_B and h , which is similar to that for one-layer structure. These can be explained by the fact that large panel height increases the heat transfer path as well as the fact that the bottom face sheet is the most effective thermal mass of the panel structure. As expected, increasing the t_{W2} leads to the enhancement of

Fig. 5 Correlation coefficients between the design parameters and the extreme responses for the one-layer (a) and two-layer (b) ITPS panels



heat short effect and thus increases the extreme back side temperature, in that the top web is directly connected with the hot side of the panel subjected to aerodynamic heating. Such information would greatly contribute to improve the understanding of influence of individual design parameter on the thermo-mechanical responses of the panels, and therefore provide greater confidence on the effects of design changes.

7.2 Optimization design results

The design results shown in Tables 7–8 and Tables 9–10 are obtained at different temperature and buckling limits by imposing all the thermo-structural constraints, for the maximum allowable deflection of 6 mm, allowable stress

in top/medium face sheet and webs of 620 MPa and in bottom face sheet of 290 MPa for the one-layer and two-layer panels, respectively. In all cases, the designed weight increases as the design constraints become more and more demanding. For one-layer structure, the values of t_B and t_W increase with increasing buckling eigenvalue limit and decreasing temperature limit. For the same temperature limit, to enhance the buckling resistance of these long sections of webs, the value of t_{W1} is increased. This causes more heat to be conducted into the panel, and thus the thermal mass and heat transfer path needs to be increased. This is done by increasing the value of t_B and h . The value of p has to decrease in order to decrease the length of the unsupported sections. This is consistent with the results provided in Ref. Bapanapalli et al. (2006). θ is at the upper bound.

Table 7 The optimization results for the one-layer ITPS panel at different minimum allowable eigenvalue limit for the maximum allowable bottom face sheet temperature of 473K

Design #	S1	S2	S3	S4
Eigenvalue limit	1.00	1.50	2.00	3.00
t_T (1-2mm)	1.19	1.19	1.22	1.98
t_B (2-8mm)	4.74	5.09	5.43	7.87
t_W (1-2mm)	1.10	1.45	1.71	2.00
θ (80-100°)	99.88	99.79	99.99	99.96
h (80-120mm)	80.78	85.94	88.79	89.93
p (22.5-112.5mm)	65.68	63.13	61.59	44.31
Mass kg/m ²	21.76	25.22	28.17	42.56
Actual $Max(T_{BFS})$ (K)	465.73	471.28	474.18	470.90
Actual $Max(D_{TFS})$ (mm)	2.93	2.58	2.37	1.44
Actual $Max(\sigma_{Ti})$ (MPa)	362.50	331.82	308.73	305.22
Actual $Max(\sigma_{Be})$ (MPa)	257.26	259.49	250.92	219.83
Actual $Min(\lambda)$	0.92	1.37	1.59	2.77

Table 8 The optimization results for the one-layer ITPS panel at different minimum allowable eigenvalue limit for the maximum allowable bottom face sheet temperature of 453K

Design #	S5	S6	S7	S8
Eigenvalue limit	1.00	1.50	2.00	3.00
t_T (1-2mm)	1.17	1.20	1.25	—
t_B (2-8mm)	5.82	6.03	6.40	—
t_W (1-2mm)	1.19	1.57	1.85	—
θ (80-100°)	99.98	99.88	99.96	—
h (80-120mm)	80.44	88.79	92.38	—
p (22.5-112.5mm)	63.52	61.78	60.54	—
Mass kg/m ²	24.25	28.24	31.63	—
Actual $Max(T_{BFS})$ (K)	450.24	454.86	456.63	—
Actual $Max(D_{TFS})$ (mm)	2.77	2.42	2.34	—
Actual $Max(\sigma_{Ti})$ (MPa)	385.55	332.19	306.16	—
Actual $Max(\sigma_{Be})$ (MPa)	135.08	251.87	247.52	—
Actual $Min(\lambda)$	0.95	1.24	1.56	—

Table 9 The optimization results for the two-layer ITPS panel at different minimum allowable eigenvalue limit for the maximum allowable bottom face sheet temperature of 473K

Design #	D1	D2	D3	D4
Eigenvalue limit	1.00	1.50	2.00	3.00
t_T (1-2mm)	1.00	1.00	1.00	1.00
t_M (1-2mm)	1.00	1.00	1.00	1.00
t_B (2-8mm)	2.00	2.13	2.62	3.44
t_{W1} (1-2mm)	1.00	1.00	1.00	1.31
t_{W2} (1-2mm)	1.00	1.00	1.00	1.00
θ_1 (80-100°)	88.65	90.45	89.66	88.71
θ_2 (80-100°)	89.40	80.76	80.20	80.08
h (80-120mm)	98.07	96.79	88.21	80.07
h_1 (5-(h-5)mm)	38.23	51.21	51.90	58.21
p (22.5-112.5mm)	112.44	112.32	112.34	112.48
Mass kg/m ²	18.62	18.81	19.16	20.79
Actual $Max(T_{BFS})$ (K)	405.10	406.07	410.62	421.22
Actual $Max(D_{TFS})$ (mm)	0.61	0.54	0.53	0.49
Actual $Max(\sigma_{Ti})$ (MPa)	332.36	342.22	339.35	358.39
Actual $Max(\sigma_{Be})$ (MPa)	71.88	68.29	70.96	58.88
Actual $Min(\lambda)$	0.75	1.10	1.63	3.01

Table 10 The optimization results for the two-layer ITPS panel at different minimum allowable eigenvalue limit for the maximum allowable bottom face sheet temperature of 453K

Design #	D5	D6	D7	D8
Eigenvalue limit	1.00	1.50	2.00	3.00
t_T (1–2mm)	1.00	1.00	1.00	1.00
t_M (1–2mm)	1.00	1.00	1.00	1.00
t_B (2–8mm)	2.32	2.74	3.24	4.14
t_{W1} (1–2mm)	1.00	1.00	1.00	1.34
t_{W2} (1–2mm)	1.00	1.00	1.00	1.00
θ_1 (80–100°)	88.76	91.42	88.08	85.74
θ_2 (80–100°)	83.21	81.95	80.04	80.45
h (80–120mm)	105.04	97.28	88.41	80.16
h_1 (5–(h–5)mm)	51.08	54.49	52.83	55.53
p (22.5–112.5mm)	112.45	112.42	112.45	112.50
Mass kg/m ²	19.65	19.94	20.30	22.14
Actual $Max(T_{BFS})$ (K)	390.46	394.54	399.24	409.06
Actual $Max(D_{TFS})$ (mm)	0.56	0.55	0.50	0.49
Actual $Max(\sigma_{Ti})$ (MPa)	332.10	344.51	337.54	345.78
Actual $Max(\sigma_{Be})$ (MPa)	69.05	70.52	68.50	56.62
Actual $Min(\lambda)$	0.86	1.18	1.67	3.01

Optimization for high buckling eigenvalue larger than 2.4 at allowable temperature limit of 453K did not produce feasible design results due to the combined requirement of temperature, buckling and stresses in bottom face sheet for the current range of variables.

For the optimization of two-layer one, the maximum thermal stress and deflection constraints become non-active because the calculated responses for most of design points are far less than the allowable values. From Tabs. 9–10, it is observed that the values of t_B and t_{W1} for two-layer structure increase with the rise of buckling eigenvalue limit and the decrease of temperature limit. The optimized design had t_{W2} , t_T and t_M at the lower bounds. For all the constraint conditions, the value of p would preferably stay at the upper bound for the two-layer structure, which means that less number of connections between panel and body structure of space vehicle is required. This could help to minimize the areal density of panel and facilitate to obtain lighter weight design of the vehicle outer structure. The values of h decrease with the rise of buckling eigenvalue limit at the same temperature limit. It is interesting to observe that the ratio of h_1 to h increases with increasing the buckling eigenvalue limit, which indicates that the medium face sheet approaching hot side in proportion is beneficial to withstand thermal buckling deformation of two-layer panel. The actual response values of each design are also shown in the corresponding tables. The error between the actual response values and the design limits in the buckling eigenvalues may be attributed to the rough response surface approximation for the two-layer corrugated panel. It is suggested that more detailed fitting model is developed in future research to improve the accuracy of response surface. Anyway, in terms

of discussing the feasibility of lowering weight from a new configuration of ITPS panel, the agreement was reasonable.

From a weight standpoint, panels with two-layer corrugated core panels are found to be more efficient for the given conditions, about 14–29 % lighter at the low thermo-mechanical constraints levels. The designed weight for the two-layer panel is 22.14 kg/m², which is about 50 % lighter than that of 42.56 kg/m² for the one-layer structure at the allowable smallest eigenvalue of 3. The two-layer structure exhibits great potential to implement lighter weight design with severe thermal buckling design requirements while obtaining more temperature, stress and deflection margins. From the thermal analysis results, it was observed that all the critical times of maximum thermal gradient occurs before 2175s, which means that the active mechanical loads for the optimization design is only the in-plane inertial compression load. Based on the derivations by Vinson (1987) and Tian (2005), the buckling stress exhibits quadratic dependence on the ratio of thickness to its length when a corrugated core sandwich panel is subjected to uniaxial compression load. The excellent thermal buckling resistance of the two-layer structure may be explained by the fact that the core is separated by the medium face sheet, which reduces the top and bottom core height, and thus the ratio of web thickness to the height of each core section increases when the web thickness is given to be constant, leading to the buckling failure stress increase. The existence of the medium face sheet separated the bottom core and top core increases the lateral heat conduction, and therefore the heat transfer from outside to inside is suppressed. Apart from that, the configuration with two layer cores contributes to increase the rigidity of the panel and resisting the

deformation of the top face sheets. These were considered as the primary mechanism to reduce the weight for the current design variable range and constraint level.

8 Conclusion

In order to determine if there is possibility to realize the weight-loss purpose through optimizing configuration of cross-sections for ITPS panel, we did a comprehensive study on the minimum-weight optimum design of two metallic corrugated core sandwich panels subjected to in-service thermal and mechanical loads by using simulated annealing algorithm, in which the geometric parameters in describing the two candidate configurations were selected as design variables, and the thermal, buckling, stress and deflection were considered as constraints of the optimization problem. Sensitivity studies were conducted to determine the influence of various design parameters on thermal and mechanical extreme responses. The results showed that the length of unit cell, height of panel, thickness of bottom face sheet and web are the most important parameters effecting on the thermo-structural extreme responses for each configuration. For the two-layer core panel, the corrugation angle of bottom core and the top web thickness also play a vital role in the smallest thermal buckling eigenvalue and peak temperature, respectively. An area-specific weight for panels with two-layer corrugated core is reduced by more than 14–29 % with respect to the one-layer core design. 30–50 % weight saving can be achieved at high thermal buckling constraints level for the two-layer structure while keeping considerable temperature, stress and deflection margins. The results demonstrate that the two-layer ITPS panel provides superior structural efficiency compared to the one-layer structure for the current considered conditions. The two-layer structure is more promising to achieve the goal of a large, thin, and low weight ITPS panel concept.

Acknowledgments This work was supported by National Natural Science Foundation of China (Grant No. 11102054 and No. 51301053), supported by Postdoctoral Science-research Developmental Foundation of Heilongjiang Province (Grant No. LBH-Q12101), supported by Fundamental Research Funds for the Central Universities (Grant No. HIT. NSRIF. 2014026).

Appendix A: Heat transfer models of ITPS (Bapanapalli et al. 2006)

The ITPS panel is subject to an incident heat flux. Re-radiation condition is applied on the top surface with an emissivity of 0.8. Convective heat loss is also applied on the top surface, after aerodynamic heating is ceased. The bottom surface is assumed to be conservative adiabatic

boundary condition. It is also assumed that there is no thermal contact resistance at the interface between the face sheets (and webs) and the insulation materials. The properties of the sandwich core are calculated using the rule of mixtures formula given below:

$$\rho_C = \frac{\rho_W t_W + \rho_S (p \sin \theta - t_W)}{p \sin \theta} \tag{7}$$

$$C_C = \frac{C_W \rho_W t_W + C_S \rho_S (p \sin \theta - t_W)}{\rho_W t_W + \rho_S (p \sin \theta - t_W)} \tag{8}$$

$$k_C = \frac{k_W t_W + k_S (p \sin \theta - t_W)}{p \sin \theta} \tag{9}$$

where C for specific heat, k for conductivity, θ for the corrugation angle. The subscripts C and W represent the homogenized core and structural web material.

The heat transfer problem is modeled as a one-dimensional thermal analysis. The governing equations and boundary conditions can be written as following.

Heat transfer equation for ITPS:

$$k_{T,C,(M),B} \frac{\partial^2 T(x, \tau)}{\partial x^2} = \rho_{T,C,(M),B} C_{T,C,(M),B} \frac{\partial T(x, \tau)}{\partial T} \tag{10}$$

$0 < t < t_{end}$

Initial condition:

$$T(x, \tau = 0) = T_i \tag{11}$$

Boundary conditions:

$$q_{out} = -k_B \frac{\partial T(x, \tau)}{\partial x} \Big|_{x=h+(t_T+t_B)/2} = 0 \tag{12a}$$

$$q_{in} = -k_T \frac{\partial T(x, \tau)}{\partial x} \Big|_{x=0} = q_i(\tau) - \varepsilon \sigma T(0, \tau)^4 - h(\tau) T(0, \tau) \tag{12b}$$

Where T is temperature, τ is time, x is location along the thickness direction, T_i is the initial temperature of the panel before atmospheric reentry, ε the emissivity of the top surface, σ is the Stefan-Boltzmann constant, $q_i(\tau)$ is the heat influx, and $h(\tau)$ is the convection coefficient at the top surface. The subscripts T, C, M and B represent the top face sheet, homogenized core, medium sheet and bottom face sheet of the ITPS panel, respectively.

Appendix B: Response surface methodology

The response surface method fits a function to a set of experimentally or numerically evaluated design data points. In

this approach, an appropriate polynomial is fitted to a set of data points by least squares method.

For a quadratic response surface approximation, the polynomial is formulated as:

$$Y = \beta_0 + \sum_{i=1}^n \beta_i X_i + \sum_{i=1}^n \beta_{ii} X_i^2 + \sum_{j=1}^n \sum_{i=1}^{j-1} \beta_{ij} X_i X_j \quad (13)$$

Where β is regression coefficient and X_i represents the i th design variables, n is the number of the design variables.

One of the most frequently used parameter to access the quality of the fitted response surface is the coefficient of multiple determination, which measures the fraction of variation in data captured by the response surface. The remaining variation is attributed to random noise. The coefficient of multiple determination R^2 is defined as

$$R^2 = \frac{\sum_{i=1}^n (\hat{Y}_i - \bar{Y})^2}{\sum_{i=1}^n (Y_i - \bar{Y})^2} \quad (14)$$

Where Y_i is the actual value of the response at the design point, \hat{Y}_i is the predicted value, and \bar{Y} is the average value of Y_i . If the R value is closer to 1, the polynomial fitted model gives a good fit. More details on the polynomial response surface approximation have been provided in Ref. Potet et al. (2004).

To evaluate the accuracy of response surface approximation, two data sets and various statistical criteria were used. The design data set includes all data points used in constructing response surface. The test data set contains n_t ($n_t = 50$ here) randomly selected points Y_i^* . The total root mean square error (RMSE) σ of response surface in the design data set is defined as

$$\sigma = \sqrt{\frac{1}{n} \sum_{i=1}^n (Y_i - \bar{Y}_i)^2} \quad (15)$$

The percentage total RMSE for the design points, designated as 'RMSE-D %', is obtained as the ratio of σ/\bar{Y} . The root mean square error in the test data (probability calculation) ε is given by the expression

$$\varepsilon = \sqrt{\frac{1}{n_t} \sum_{i=1}^{n_t} (Y_i^* - \bar{Y}_i)^2} \quad (16)$$

The percentage total RMSE for the test points, designated as 'RMSE-T %', is obtained as the ratio of ε/\bar{Y} . If this value is close to zero then the model performs well.

Appendix C: Correlation coefficient method

The correlation coefficient r is given by

$$r = \frac{\sum_{i=1}^n (X_i - \bar{X})(Y_i - \bar{Y})}{\sqrt{\sum_{i=1}^n (Y_i - \bar{Y})^2} \sqrt{\sum_{i=1}^n (X_i - \bar{X})^2}} \quad (17)$$

Where \bar{X} represents the mean value of input variables. The correlation coefficient can be interpreted as the fractional contribution to the uncertainty in the output due to uncertainty in a given input parameter. The magnitude of the correlation coefficient provides a way to rank the importance of the individual physical variables. If the absolute value of correlation coefficient is close to unity, the parameter strongly affects the response. On the other hand, if the correlation coefficient is close to zero, the parameter has little contribution to the response. Evaluating the correlation coefficients can therefore offer good insight into the mechanism of the response.

References

- Alrefaei MH, Diabat AH (2009) A simulated annealing technique for multi-objective simulation optimization. *Appl Math Comput* 215:3029–3035
- Aryanezhad MB, Hemati M. (2008) A new genetic algorithm for solving nonconvex nonlinear programming problems. *Appl Math Comput* 199:186–194
- Bapanapalli SK, Martinez OM, Gogu C, Sankar BV, Haftka RT (2006) Analysis and design of corrugated-core sandwich panels for thermal protection systems of space vehicles. 47th AIAA/ASME/ASCE/AHS/ASC Structures, structural dynamics, and materials conference AIAA 1942
- Bapanapalli SK (2007) Design of an integrated thermal protection system for future space vehicles. Ph.D. dissertation. University of Florida
- Clarke S, Griebisch JH, Simpson LT (2005) Analysis of support vector regression for approximation of complex engineering analyses. *Transactions of ASME, Journal of Mechanical Design* 127(9):1077–1087
- Daxner T, Flatscher T, Rammerstorfer FG (2007) Optimum design of corrugated board under buckling constraints. In: 7th world congress on structural and multidisciplinary optimization COEX Seoul
- Erdal O, Sonmez FO (2005) Optimum design of composite laminates for maximum buckling load capacity using simulated annealing. *Compos Struct* 71:45–52
- Gogu C, Bapanapalli SK, Haftka RT, Sankar BV (2009) Comparison of materials for an integrated thermal protection system for spacecraft reentry. *J Spacecr Rocket* 46(3):501–513
- Harlod SZU, Hartley R (1987) Fast simulated annealing. *Phys Lett (A)* 122(3,4):157–162
- Hastie T, Tibshirani R, Friedman J (2001) The elements of statistical learning: data mining, inference, and prediction. Springer
- Khalkhali A, Asadi H, Gorji M, Ashouri. D (2007) Modeling and optimization of sandwich panels with corrugated cores. In:

- 3rd WSEAS international conference on applied and theoretical mechanics:60–66
- Kirkpatrick S, Gelatt CD, Vecchi MP (1983) Optimization by Simulated Annealing. *Science* 220:671–680
- Kumar S, Villanueva D, Sankar BV, Haftka RT (2008) Probabilistic optimization of integrated thermal protection system. 12th AIAA/ISSMO multidisciplinary analysis and optimization conference AIAA 5928
- Liang CC, Yang MF, Wu PW (2001) Optimum design of metallic corrugated core sandwich panels subjected to blast loads. *Ocean Eng* 28:825–861
- Lombardi M, Hafta RT, Cinquini C (1992) Optimization of composite plates for buckling by simulated annealing. AIAA-92-2313-CP
- Mageras GS, Mohan R (1993) Application of fast simulated annealing to optimization of conformal radiation treatments. *Med Phys* 20(3):639647
- Martin JD, Simpson TW (2005) Use of kriging models to approximate deterministic computer models. *AIAA J* 43(7):853–863
- Martinez O. (2007) Micromechanical analysis and design of an integrated protection system for future space vehicles. Ph.D. dissertation. University of Florida
- Metropolis N, Rosenbluth A, Rosenbluth M, Teller A, Teller E. (1953) Equation of state calculations by fast computing machines. *J Chem Phys* 21:1087–092
- Miller I, Freund JE, Johnson RA (1965) Probability and statistics for engineers, vol 4. Prentice-Hall, Englewood Cliffs, p 432
- Myers RH, Montgomery DC (1995) Response surface methodology: process and product optimization using designed experiments. John Wiley, New York
- Olamaei J, Niknam T, Gharehpetian G (2008) Application of particle swarm optimization for distribution feeder reconfiguration considering distributed generators *Applied. Math Comput* 201:575–586
- Pichona T, Barreteau R, Soyris P, Foucault A, Parenteau JM, Prel Y, Guedron S. CMC (2009) thermal protection system for future reusable launch vehicles: Generic shingle technological maturation and tests. *Acta Astronautica* 165176:65
- Poteet CC, Hasan AK, Hsu SY (2004) Preliminary thermal-mechanical sizing of a metallic thermal protection system. *J Spacecr Rocket* 41(2):173–182
- Ravishankar B, Sankar BV, Haftka RT (2011) Uncertainty analysis of integrated thermal protection system with rigid insulation bars. 52nd AIAA/ASME/ASCE/AHS/ASC structures, structural dynamics and materials conference AIAA 1767
- Sharma A, Gogu C, Martinez OA, Sankar BV, Haftka RT (2008) Multi-fidelity design of an integrated thermal protection system for spacecraft reentry. 49th AIAA/ASME/ASCE/AHS/ASC structures, structural dynamics, and materials conference AIAA 2062
- Savsani V, Rao RV, Vakharia DP (2010) Optimal weight design of a gear train using particle swarm optimization and simulated annealing algorithms. *Mech Mach Theory* 45:531–541
- Shi Y, Eberhart R (1998) A modified particle swarm optimizer. *International Conference Evolutionary Computation*:69–73
- Shieh HL, Kuo CC, Chiang CM (2011) Modified particle swarm optimization algorithm with simulated annealing behavior and its numerical verification. *Appl Math Comput* 218:4365–4383
- Tian YS, Lu TJ (2005) Optimal design of compression corrugated panels. *Thin-Walled Struct* 43:477–498
- Villanueva D, Haftka RT, Sankar BV (2010) Including future tests in the design of an integrated thermal protection system. 51st AIAA/ASME/ASCE/AHS/ASC structures, structural dynamics, and materials conference AIAA 2597
- Vinson JR (1987) Minimum weight web-core sandwich panels subjected to combined uniaxial compression and in-plane shear loads. AIAA/ASME/ASCE/AHS 28th structures. *Structural Dynamics and Material Conference* 0768:282–288
- Vinson JR, Shore S (1971) Minimum weight web core sandwich panels subjected to uniaxial compression. *AIAA J Aircr* 8:843–847
- Wang L, Zheng DZ (2000) Simulated Annealing with the State Generator Based on Cauchy and Gaussian Distributions. *J Tsinghua Univ (Sci Tech)* 40(9):109–112
- Xu SL (2004) C algorithms commonly used procedures set, 3rd edn. Tsinghua University Press, pp 351–363